

Citation for published version:

Ó. López *et al.*, "Eliminating Ground Current in a Transformerless Photovoltaic Application," in *IEEE Transactions on Energy Conversion*, vol. 25, no. 1, pp. 140-147, March 2010, doi: 10.1109/TEC.2009.2037810.

Peer reviewed version

Link to published version: [10.1109/TEC.2009.2037810](https://doi.org/10.1109/TEC.2009.2037810)

General rights:

© 2010 IEEE. Personal use of this material is permitted. Permission from IEEE must be obtained for all other uses, in any current or future media, including reprinting/republishing this material for advertising or promotional purposes, creating new collective works, for resale or redistribution to servers or lists, or reuse of any copyrighted component of this work in other works.

Eliminating Ground Current in a Transformerless Photovoltaic Application

Oscar López, *Member, IEEE*, Francisco D. Freijedo, *Member, IEEE*, Alejandro G. Yepes, *Student Member, IEEE*, Pablo Fernández-Comesaña, *Student Member, IEEE*, Jano Malvar, *Student Member, IEEE*, Remus Teodorescu, *Senior Member, IEEE*, and Jesús Doval-Gandoy, *Member, IEEE*

Abstract—For low-power grid-connected applications, a single-phase converter can be used. In photovoltaic (PV) applications, it is possible to remove the transformer in the inverter to reduce losses, costs, and size. Galvanic connection of the grid and the dc sources in transformerless systems can introduce additional ground currents due to the ground parasitic capacitance. These currents increase conducted and radiated electromagnetic emissions, harmonics injected in the utility grid, and losses. Amplitude and spectrum of the ground current depend on the converter topology, the switching strategy, and the resonant circuit formed by the ground capacitance, the converter, the ac filter, and the grid. In this paper, the ground current in a 1.5-kW PV installation is measured under different conditions and used to build a simulation model. The installation includes a string of 16 PV panel, a full-bridge inverter, and an LCL filter. This model allows the study of the influence of the harmonics injected by the inverter on the ground current.

Index Terms—Ground current, photovoltaic (PV) power systems, pulsewidth-modulated inverters, single-phase system, utility interface.

I. INTRODUCTION

AS DISTRIBUTED power sources become increasingly prevalent in the near future, power electronics will be able to provide significant advantages in processing power from renewable energy sources using fast response and autonomous control [1], [2]. Fuel cells, photovoltaic (PV) devices, and storage battery sources produce low voltages, so a dc–dc boost converter is generally required to adapt the voltage level for the grid-connected inverter. This dc–dc converter, in addition to boosting, also regulates the inverter input voltage and sometimes isolates the low- and high-voltage circuits.

Most of the commercially available converters for renewable applications include a transformer, which enables the selection of a suitable dc voltage input for the inverter and isolates the energy source from the utility grid [3]. Converters including a transformer either use a line transformer or a high-frequency transformer. Line-frequency transformers are regarded as poor

components due to increased size, weight, and prize. Converters with high-frequency transformers include various power stages and are pretty complex. Transformerless concept is advantageous regarding their high efficiencies reached of up to 97%–98%, which is highly attractive for distributed power generator systems [4]–[7]. Avoiding the transformer has the additional benefits of reducing cost, size, weight, and complexity of the inverter. However, the removal of the transformer, and hence its isolation capability, has to be considered carefully. An analysis of different standards shows that the PV panels must be ever grounded in USA [8], and only under certain conditions in Europe [9]. When grounding of the PV panels frame is a requirement, the PV ground parasitic capacitance needs to be considered in transformerless topologies. Because of the capacitance between the PV panels and ground, potential differences imposed by switching actions of the inverter inject a capacitive ground current [10]. This ground capacitance is part of a resonant circuit consisting of the PV panels, the ac filter elements, and the grid impedance [11]. Because of necessary efficiency optimization of systems, the damping of this resonant circuit can be very small, so that the ground current can reach amplitudes well above permissible levels. Also, the resonant frequency is not fixed due to the ground capacitance dependence on environmental conditions. Depending on the topology and the switching strategy, the ground current can cause more or less severe (conducted and radiated) electromagnetic interferences, grid current distortion, and additional losses in the system [12], [13].

This paper evaluates the ground current in a full-bridge single-phase transformerless inverter connected to the grid [14]. Ground voltage and currents were measured in a 1.5-kW PV installation using unipolar and bipolar modulation strategies. Ground current differences between both strategies are discussed. From these experimental results, the value of the ground capacitance is estimated and a model of the resonant circuit is presented. The simulation results are compared with the experimental results, and the resonance frequency of the system is calculated using this model. Finally, in order to eliminate ground current in transformerless installations, the substitution of the usual full-bridge inverter for a neutral point clamped (NPC) topology is discussed [15].

II. FULL-BRIDGE TOPOLOGY

The topology shown in Fig. 1 is a standard full-bridge voltage source inverter. Different pulsewidth modulation (PWM)

Manuscript received June 4, 2008; revised March 25, 2009. First published January 29, 2010; current version published February 17, 2010. This paper was presented at the 2007 Power Engineering Society General Meeting, Tampa, FL, June 24–28. This work was supported by the Spanish “Ministerio de Ciencia e Innovación” under Project DPI2009-07004. Paper no. TEC-00213-2008.

O. López, F. D. Freijedo, A. G. Yepes, P. Fernández-Comesaña, J. Malvar, and J. Doval-Gandoy are with the Department of Electronics Technology, University of Vigo, Vigo 36310, Spain (e-mail: olopez@uvigo.es).

R. Teodorescu is with the Institute of Energy Technology, Aalborg University, Aalborg 9220, Denmark (e-mail: ret@iet.aau.dk).

Color versions of one or more of the figures in this paper are available online at <http://ieeexplore.ieee.org>.

Digital Object Identifier 10.1109/TEC.2009.2037810

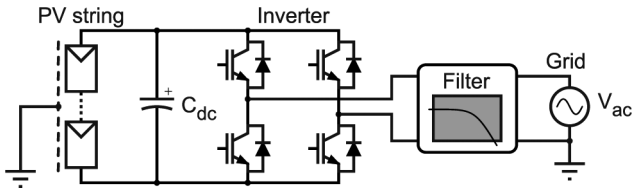


Fig. 1. Voltage source PV transformerless inverter connected to the grid.

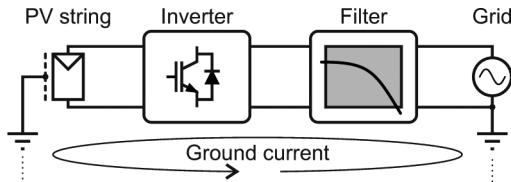


Fig. 2. Ground current in a PV transformerless inverter connected to the grid.

switching patterns can be used in transformerless single-phase inverter bridges. By using bipolar PWM, the diagonal switch pairs are fired alternately and the bridge voltage changes between $+V_{dc}$ and $-V_{dc}$. In order to reduce the losses, unipolar PWM is commonly used. Using this switching strategy, the bridge voltage output has three possible levels: $+V_{dc}$, 0, and $-V_{dc}$. Unipolar PWM has various advantages over bipolar PWM. Ripple current is significantly less because of the three-level switching pattern that reduces filtering requirements. Unipolar PWM changes the voltage across the inductor by V_{dc} for each switch transition, which implies that the dv/dt is reduced. This results in lower switching losses, lower switch stresses, and reduced electromagnetic emissions.

III. GROUND CURRENT AND RESONANCE FREQUENCY

Without transformer, there is a galvanic connection of the grid and the dc source, and thus, a ground current appears [16]. Disadvantages of the appearing ground current are increased system losses, impairing of electromagnetic compatibility, and safety problems [17]. Ground current is limited by standards. For instance, in Germany [9], every PV system needs to include a residual current monitoring unit (RCMU), which observes the ground current, and if it is greater than 300 mA, the system must be disconnected in 0.3 s.

In general, the ground current is superimposed to the line current; therefore, the harmonic content is increased compared with inverters without the transformer. In the transformerless grid-connected system shown in Fig. 2, a resonant circuit is created if the dc generator is grounded. This resonant circuit includes the ground capacitance, the filters, the inverter, and the impedance of the connected utility grid. Magnitude of the mentioned capacitance depends on the dc source and the environmental conditions. For fuel cells, this ground capacitance is very small, so ground currents with this kind of sources is not a topic. Nevertheless, ground capacitance of PV panels can be

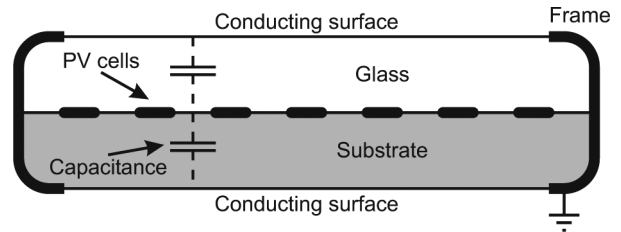


Fig. 3. PV panels ground capacitance.

very high; it goes from nanofarads up to microfarads [10], [11], because PV panel structure is like a huge capacitor, where one electrode is formed by the PV cells and the other by the grounded frame (see Fig. 3). Therefore, ground current can reach high levels, thus becoming an important issue in transformerless PV applications.

It is important to know the resonance frequency in order to get a properly working system, because the first measure to reduce the ground currents is to decrease the excitation of the resonant circuit. A problem arises due to the great dependence of the ground capacitance with environmental conditions, and hence the resonance frequency of the system. The resonance of the system can be controlled by a damping resistor or the choice of the LCL filter.

IV. EXPERIMENTAL RESULTS

The PV power system consists of a string of 16 BP MSX 120 PV panels, a full-bridge voltage source inverter, and an LCL grid filter. Each panel has a nominal power of 120 W and an open-circuit voltage of 42.1 V.

A 915- μF electrolytic capacitor is used for the power decoupling between the PV modules and the single-phase grid. The inverter is made using the power stage of the commercial converter Danfoss VLT 5004 rated 400 V/10 A. The output of the filter is directly connected to the grid without insulation transformer. The parameters of the LCL filter are: $C_f = 2.2 \mu\text{F}$, $L_f = 1426 \mu\text{H}$ and $L_i = 713 \mu\text{H}$. The effective switching frequency in the filter is 20 kHz; therefore, when unipolar modulation is used, the inverter switching frequency must be 10 kHz. The control algorithm was implemented using the dSPACE DS1103 platform [18]. The main elements of the PV control structure are:

- 1) the synchronization system using a phase-locked loop;
- 2) the input power control using a dc voltage controller with a power feedforward loop;
- 3) the grid current controller using the proportional resonant controller with harmonic compensation for the third, fifth, seventh, and ninth harmonics [19].

A maximum power point tracking (MPPT) algorithm was not used in order to analyze the system ground current under different power output conditions. In all cases analyzed, the PV panels worked at almost constant sun irradiation of 1050 W/m^2 . Fig. 4 shows the voltage and current output waveforms with the

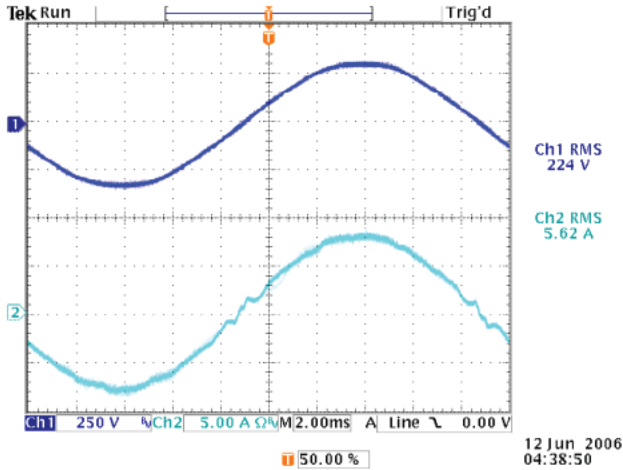


Fig. 4. Grid voltage (Ch#1) and grid current injected (Ch#2) waveforms.

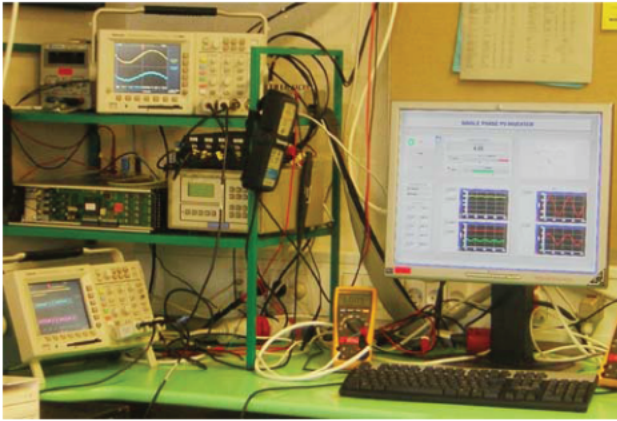


Fig. 5. Setup photograph.

system supplying 1.26 kW to the grid. A photograph of the experimental setup is shown in Fig. 5.

Fig. 6 compares the measured ground voltage and ground current for unipolar and bipolar modulations when the system is delivering 0 and 1260 W to the utility grid. The modulation strategy has the main influence on the ground voltage and hence on the ground current. With bipolar modulation, the ground voltage has a sinusoidal waveform with an amplitude of $V_{ac}/2$ at line frequency. With unipolar modulation, the ground voltage has superimposed a high-frequency signal to this sinusoidal waveform. Therefore, in this case, the ground current is much higher, as it can be seen comparing the left and the right waveforms in Fig. 6. The power output of the converter seems to be also influence on the ground current when unipolar modulation is used. This is an indirect influence due to the fact that the amplitude of the high-frequency component of the ground voltage depends on the amplitude of the dc bus. And the amplitude of the dc bus does not stand constant because the PV panels voltage output depends greatly on the power that they are delivering. Table I shows the characteristics of the PV panels used.

Spectral analysis of ground voltage and ground current in the unipolar modulation case gives the results, displayed in Fig. 7. As expected, high-frequency components appear. In particular, only the odd multiples of the switching frequency (10, 30, 50, 70, 90 kHz, etc.) are present because the even multiples are blocked by the output filter. Amplitude of the 70 kHz harmonic is the largest one, as shown in Fig. 7; hence, the system has a resonance peak near to this frequency. When bipolar modulation is used, there are no high-frequency harmonic components in the ground voltage [12]; therefore, in this case, the resonant circuit is not excited and the resonance is not a problem.

Table II shows the amplitude of the main components of ground voltage and ground current under different operational conditions. Only the harmonics detailed in this table could be measured with reasonable accuracy. From each pair of values of voltage V_{C_p} and current I_{C_p} , a value for the ground capacitance C_p was estimated as follows:

$$C_p = \frac{1}{2\pi f} \frac{I_{C_p}}{V_{C_p}}. \quad (1)$$

It is important to remark that values calculated with low-frequency harmonics are very different from those obtained from high-frequency harmonics. Bipolar modulation does not have high-frequency harmonics, and therefore, the capacity calculated in this case is not suitable to be considered for a high-frequency model. For the high-frequency components, the value of the ground capacitance estimated is 13.6 nF, it means 7.08 nF/kW. This value was obtained as the average of the C_p calculated values from the unipolar row of Table II.

V. SIMULATION MODEL

On the basis of the previous experimental results, the model shown in Fig. 8 was built to study the ground current and calculate the resonance frequency of the system. The model includes a capacitor C_p that models the parasitic ground capacitance. In order to compare the simulation results with the experimental measurements, the same cases studied in the previous section have been simulated. Hence, values of parameters displayed in Table III together with unipolar and bipolar modulation strategies were used in the simulations. Voltage of the dc source that models the PV panels was taken, accordingly with the power output, from Table I. All simulations were made using the PLECS toolbox, which allows fast simulation of power electronic circuits under Simulink. This toolbox provides the environment for modeling large power electronic systems containing both electrical circuits and controllers. Similarity between the simulation waveforms shown in Fig. 9 and the experimental results shown in Fig. 6 validates the proposed model.

The circuit shown in Fig. 10, derived from circuit shown Fig. 8, is proposed to study the frequency response of the resonant system. Fig. 11 shows the Bode plot of the transfer function that relates ground current to the voltage harmonics injected by

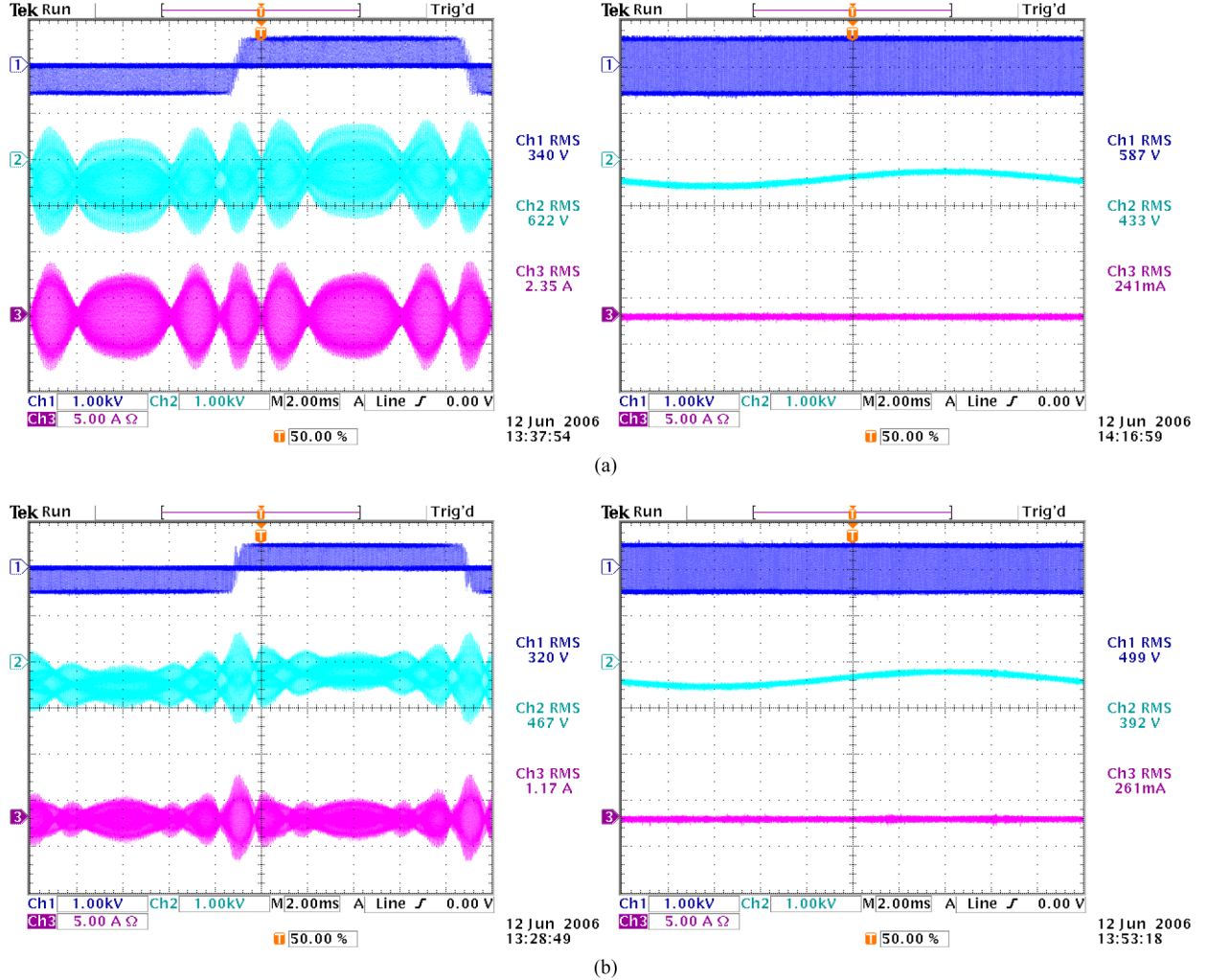


Fig. 6. Measured ground voltage and ground current with unipolar and bipolar PWM (Ch#1: inverter output, Ch#2: ground voltage, Ch#3: ground current). (a) $P = 0$ W. (b) $P = 1260$ W.

TABLE I
VOLTAGE OUTPUT OF THE PV PANELS AT 1050 W/m² IRRADIATION

Power (W)	Current (A)	Voltage (V)
0	0.0	600
630	1.1	571
1260	2.5	512

the converter, i.e.,

$$H(s) = \frac{I_h(s)}{V_h(s)}.$$

This plot presents a maximum at 70.4 kHz, which is near to the 70 kHz frequency, as it was appointed in the previous section. Therefore, the high-frequency capacitance of the panels is well estimated.

Assuming that the grid inductance L is much smaller than the filter inductance L_f and the cutoff frequency of the filter is much smaller than the resonant frequency of the system, an

approximate value of the resonance frequency can be calculated by means of the following expression:

$$f_r = \frac{1}{\pi \sqrt{L_f C_p}}. \quad (2)$$

Using this equation, the calculated resonance frequency of the system is 72.3 kHz, which is closer to the resonance frequency of the Bode plot. At this frequency obtained analytically, a large ground current appears in the PV panels.

VI. NPC TOPOLOGY

Multilevel technology provides alternative solutions to make the connection of PV panels to the grid without the transformer. The model shown in Fig. 12 was used to simulate the previous installation if the full-bridge inverter is substituted by an NPC inverter. NPC inverters [20], [21] provide multiple voltage levels through the connection of the output terminal to the nodes of a series bank of dc sources. Full-bridge inverter with

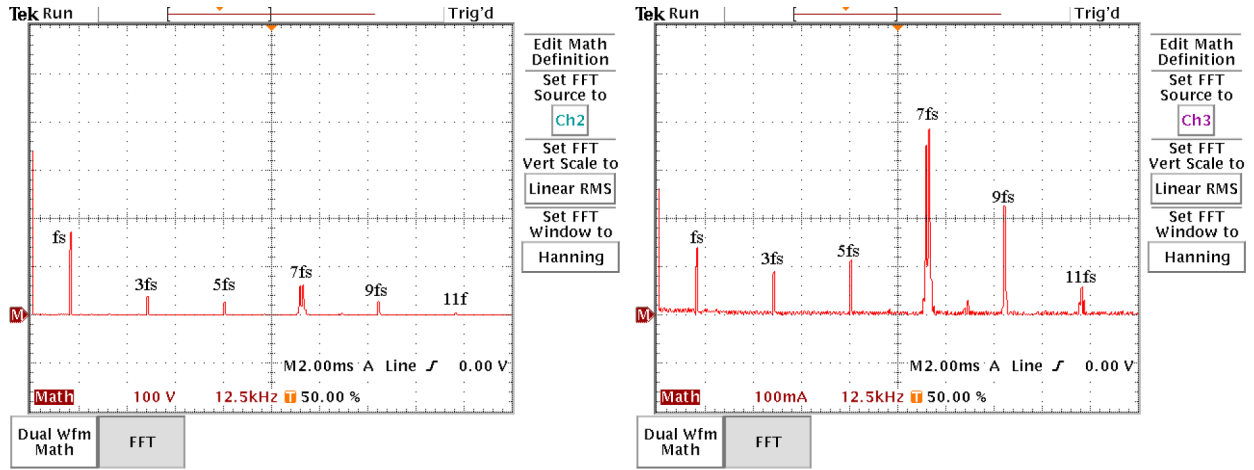


Fig. 7. Voltage and current spectrum with unipolar PWM.

TABLE II
CAPACITANCE ESTIMATION

Modulation type	Output power P (W)	Harmonic frequency f (Hz)	Ground voltage V_{C_p} (V)	Ground current I_{C_p} (mA)	C_p (nF)
Unipolar	0	10000	226	180	12,7
		30000	46	110	12,7
		50000	40	160	12,7
		70000	192	1160	13,7
		90000	10	100	17,7
	630	10000	210	156	11,8
		30000	46	100	11,5
		50000	30	112	11,9
		70000	118	692	13,3
		90000	16	136	15,0
1260	10000	174	138	12,6	
	30000	28	88	16,7	
	50000	26	112	13,7	
	70000	62	384	14,1	
	90000	30	126	7,4	
Bipolar	0	50	110	10	296
	630	50	112	11	320
	1260	50	110	6	179

unipolar PWM and NPC inverter have many similarities. They both have the same number of controlled switches, they can create the same three-level output, the effective switching frequency doubles semiconductor switching frequency, and they have similar dv/dt . Therefore, both inverters have the same filter requirements, the same current ripple, and similar switching stress.

The main advantage of the NPC inverter is that the midpoint of the dc sources is connected to the neutral of the grid. Therefore, as Fig. 13 shows, the ground voltage is nearly constant that eliminates ground current. It makes this topology very attractive for

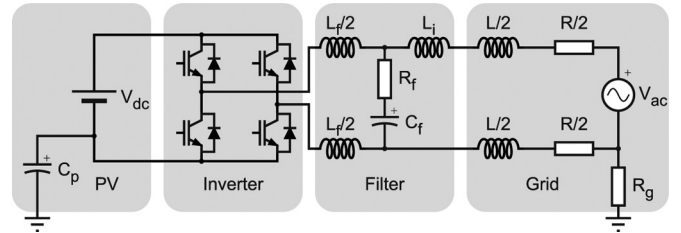


Fig. 8. Simulation model of the PV inverter.

TABLE III
GRID AND FILTER PARAMETERS

Parameter	Value
V_{ac}	224 V
f	50 Hz
L	0.04 mH
R	0.1 Ω
R_g	10 Ω
L_f	1.426 mH
C_f	2.2 μ F
R_f	1 Ω
L_i	0.713 mH
C_p	13.6 nF

transformerless single-phase grid-connected applications with high dc ground capacitance like PV panels.

Main drawbacks of the NPC inverter are that it needs two PV strings, which are loaded only during half line cycle. This requires enlarged decoupling capacitors, which increase the cost and the size of the converter. In addition, the operation of each PV strings at the maximum power point makes the system control more difficult.

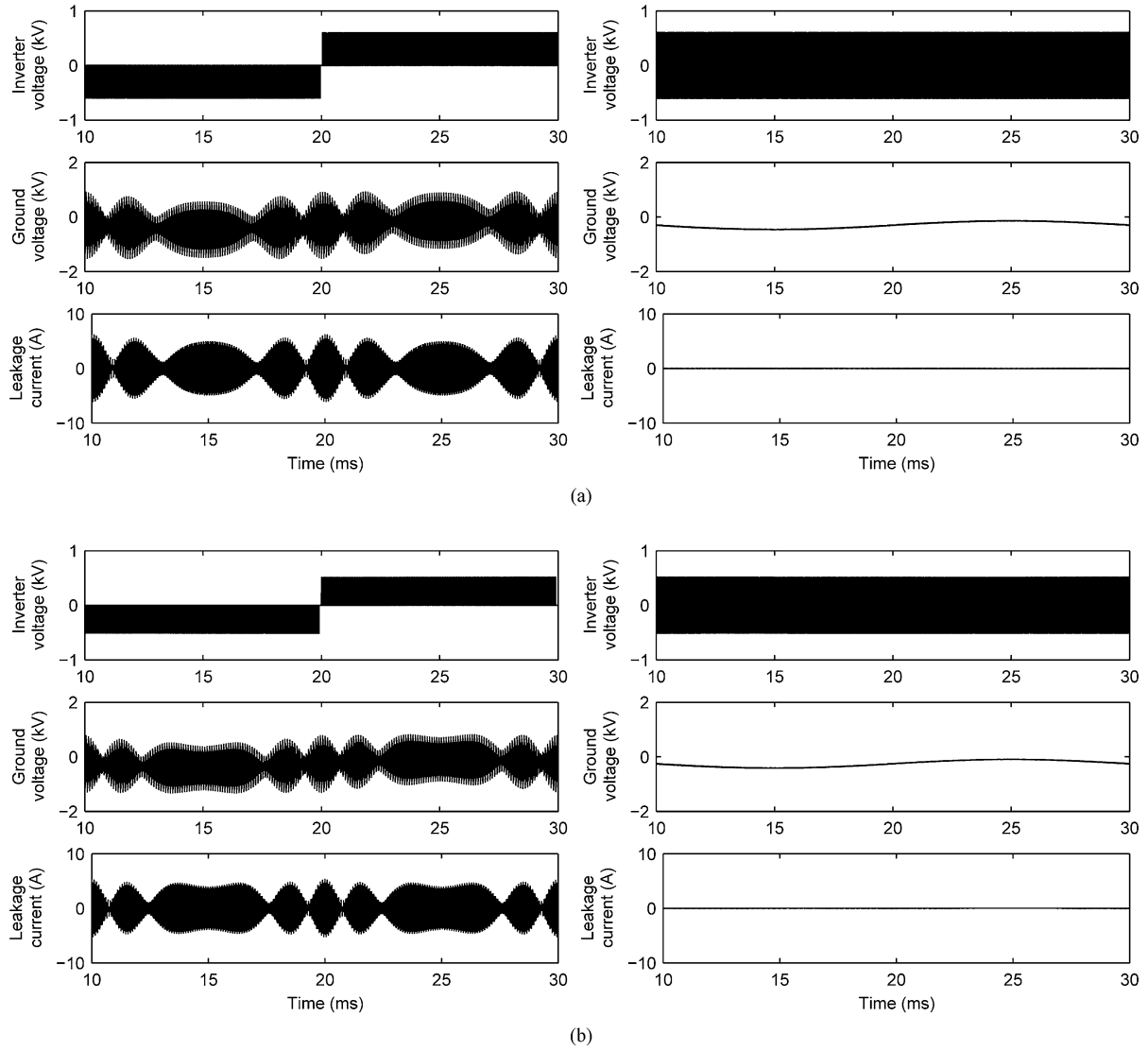


Fig. 9. Simulated ground voltage and ground current with unipolar and bipolar PWM. (a) $P = 0$ W. (b) $P = 1260$ W.

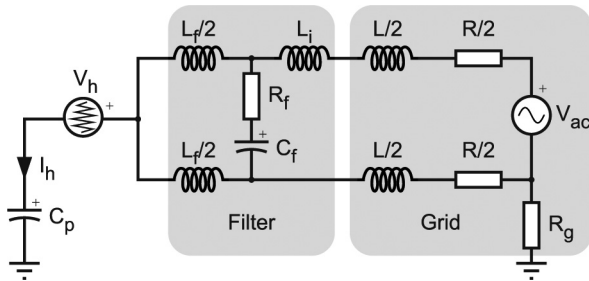


Fig. 10. Model of the resonant circuit.

Table IV compares both topologies in terms of modulation strategy, output levels, filter requirements, switches count, commutation and voltage stress, control complexity ground voltage, and ground current.

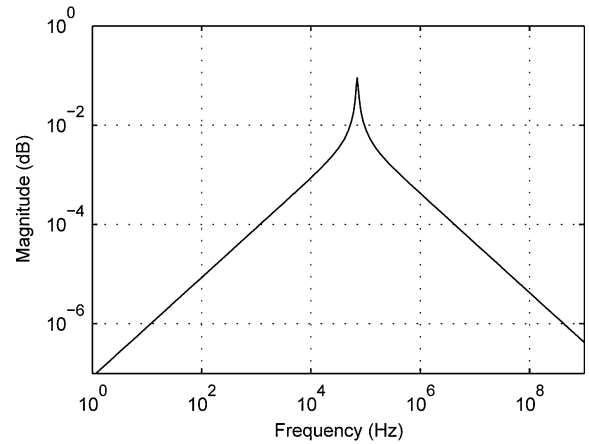


Fig. 11. $H(s)$ Bode plot of the resonant circuit model.

TABLE IV
COMPARATIVE

Topology	Output levels	Switches count	Commutation stress	Voltage stress	Filter requirements	Control complexity	Ground voltage	Ground current
Full Bridge (bipolar)	2	4	1	1	Medium	Low	Medium	Low
Full Bridge (unipolar)	3	4	0.5	1	Low	Low	High	High
Neutral Point Clamped	3	4+2	1	0.5	Low	High	Very low	Very low

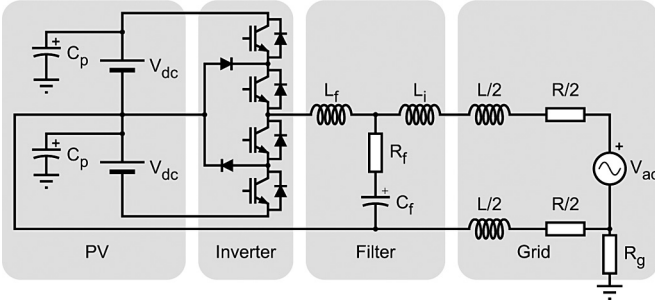


Fig. 12. Simulation model of the NPC PV inverter.

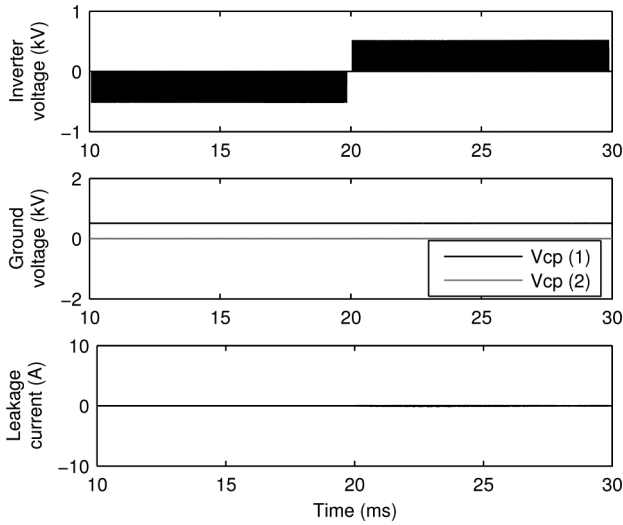


Fig. 13. Simulated ground voltage and ground current with an NPC inverter.

VII. CONCLUSION

In this paper, the ground current in a single-phase transformerless inverter connected to the grid was evaluated. Waveforms of the measured ground voltage and ground current with different modulation strategies and under different output power conditions are presented. Without the isolation capabilities of the transformer, a resonant circuit arises due to the ground capacitance of the PV panels. The study of the ground current spectrum shows the existence of the resonant frequency in the system. Dependency of the ground current on dc bus amplitude, modulation strategy, switching frequency, and filter LCL choosing was appointed. Modulation strategy has the main influence on the ground current. Bipolar modulation causes much lower ground current than unipolar modulation; so, in this case, the resonant frequency is not a problem.

On the basis of the experimental results, the ground capacitance of the PV panels was estimated and a simple model that produces similar results was built. From this, a resonant circuit model was proposed and an expression to calculate the approximate resonance frequency of the system was derived. Values estimated for ground capacitance change with frequency, so further investigation in this topic is needed in order to obtain an improved model that provide accurate results.

Neutral point clamped inverter has low current ripple, low filter requirements, low switching losses, and low switches stress, but without the ground current problem. Elimination of ground current makes this topology very interesting for single-phase grid-connected applications, where dc sources present high ground capacitance. PV inverters are included in these applications.

REFERENCES

- [1] S.-H. Ko, S. Lee, H. Dehbonei, and C. Nayar, "Application of voltage- and current-controlled voltage source inverters for distributed generation systems," *IEEE Trans. Energy Convers.*, vol. 21, no. 3, pp. 782–792, Sep. 2006.
- [2] F. Blaabjerg, Z. Chen, and S. Kjaer, "Power electronics as efficient interface in dispersed power generation systems," *IEEE Trans. Power Electron.*, vol. 19, no. 5, pp. 1184–1194, Sep. 2004.
- [3] S. Kjaer, J. Pedersen, and F. Blaabjerg, "A review of single-phase grid-connected inverters for photovoltaic modules," *IEEE Trans. Ind. Appl.*, vol. 41, no. 5, pp. 1292–1306, Sep./Oct. 2005.
- [4] D. Casadei, G. Grandi, and C. Rossi, "Single-phase single-stage photovoltaic generation system based on a ripple correlation control maximum power point tracking," *IEEE Trans. Energy Convers.*, vol. 21, no. 2, pp. 562–568, Jun. 2006.
- [5] R. Gonzalez, R. Gonzalez, J. Lopez, P. Sanchis, and L. Marroyo, "Transformerless inverter for single-phase photovoltaic systems," *IEEE Trans. Power Electron.*, vol. 22, no. 2, pp. 693–697, Mar. 2007.
- [6] R. Gonzalez, E. Gubia, J. Lopez, and L. Marroyo, "Transformerless single-phase multilevel-based photovoltaic inverter," *IEEE Trans. Ind. Electron.*, vol. 55, no. 7, pp. 2694–2702, Jul. 2008.
- [7] T.-F. Wu, T.-F. Wu, H.-S. Nien, H.-M. Hsieh, and C.-L. Shen, "PV power injection and active power filtering with amplitude-clamping and amplitude-scaling algorithms," *IEEE Trans. Ind. Appl.*, vol. 43, no. 3, pp. 731–741, May/June 2007.
- [8] *IEEE Recommended Practice for Utility Interface of Photovoltaic (PV) Systems*, IEEE Standard 929, 2000.
- [9] *Automatic Disconnection Device between a Generator and the Public Low-Voltage Grid*, DIN Electrotechnical Standard DIN VDE 0126-1-1, 2005.
- [10] M. Calais, V. G. Agelidis, and M. Meinhardt, "Multilevel converters for single-phase grid connected photovoltaic systems: An overview," *Solar Energy*, vol. 66, no. 5, pp. 325–335, Aug. 1999.
- [11] M. Meinhardt and P. Mutschler, "Inverters without transformer in grid connected photovoltaic applications," in *Proc. Eur. Conf. Power Electron. Appl. EPE*, Sevilla, Spain, Sep. 1995, vol. 3, pp. 3086–3091.
- [12] O. López, J. Doval-Gandoy, C. M. Peñalver, J. Rey, and F. D. Freijedo, "Redundancy and basic switching rules in multilevel converters," *Int. Rev. Electr. Eng.*, pp. 66–73, Jan./Feb. 2006.

- [13] T. Kerekes, R. Teodorescu, and U. Borup, "Transformerless photovoltaic inverters connected to the grid," in *Proc. IEEE Appl. Power Electron. Conf. (APEC)*, Anaheim, CA, Feb. 25–Mar. 1, 2007, pp. 1733–1737.
- [14] T.-F. Wu, T.-F. Wu, H.-S. Nien, C.-L. Shen, and T.-M. Chen, "A single-phase inverter system for PV power injection and active power filtering with nonlinear inductor consideration," *IEEE Trans. Ind. Appl.*, vol. 41, no. 4, pp. 1075–1083, Jul./Aug. 2005.
- [15] H. Hinz and P. Mutschler, "Single phase voltage source inverters without transformer in photovoltaic applications," in *Proc. Int. Power Electron. Motion Control Conf. (PEMC)*, Budapest, Hungary, Sep. 2–4, 1996, vol. 3, pp. 161–165.
- [16] T. Kerekes, R. Teodorescu, C. Klumpner, M. Sumner, D. Florica, and P. Rodriguez, "Evaluation of three-phase transformerless photovoltaic inverter topologies," in *Proc. Eur. Conf. Power Electron. Appl. EPE*, Aalborg, Denmark, Sep. 2–5, 2007, pp. 1–10.
- [17] J. Myrzik and M. Calais, "String and module integrated inverters for single-phase grid connected photovoltaic systems—A review," presented at the IEEE Power Tech., Bologna, Italy, Jun. 23–26, 2003, vol. 2.
- [18] M. Ciobotaru, R. Teodorescu, and F. Blaabjerg, "Control of single-stage single-phase PV inverter," in *Proc. Eur. Conf. Power Electron. Appl. EPE*, Dresden, Germany, Sep. 11–14, 2005, p. 10.
- [19] R. Teodorescu, F. Blaabjerg, U. Borup, and M. Liserre, "A new control structure for grid-connected LCL PV inverters with zero steady-state error and selective harmonic compensation," in *Proc. IEEE Appl. Power Electron. Conf. Expo. (APEC)*, 2004, vol. 1, pp. 580–586.
- [20] A. Nabae, I. Takahashi, and H. Akagi, "A new neutral-point-clamped PWM inverter," *IEEE Trans. Ind. Appl.*, vol. IA-17, no. 5, pp. 518–523, Sep./Oct. 1981.
- [21] F. Wang, "Reduce beat and harmonics in grid-connected three-level voltage-source converters with low switching frequencies," *IEEE Trans. Ind. Appl.*, vol. 43, no. 5, pp. 1349–1359, Sep./Oct. 2007.



Óscar López (M'05) received the M.Sc. and Ph.D. degrees from the University of Vigo, Vigo, Spain, in 2001 and 2009, respectively.

Since 2004, he has been an Assistant Professor in the Department of Electronics Technology, University of Vigo. His research interests include ac power switching converters technology.



Francisco D. Freijedo (M'07) received the M.Sc. degree in physics from the University of Santiago de Compostela, Santiago de Compostela, Spain, in 2002, and the Ph.D. degree from the University of Vigo, Vigo, Spain, in 2009.

Since 2005, he has been an Assistant Professor in the Department of Electronics Technology, University of Vigo. His research interests include quality problems, grid-connected switching converters, ac power conversion, and flexible ac transmission systems.



Alejandro G. Yepes (S'09) received the M.Sc. degree in 2009 from the University of Vigo, Vigo, Spain, where he is currently working toward the Ph.D. degree in the Department of Electronic Technology.

Since 2008, he has been in the Department of Electronics Technology, University of Vigo. His research interests include switching power converters, grid-connected converters, control of ac drives, and power quality problems.



Pablo Fernández-Comesaña (S'09) received the M.Sc. degree in 2007 from the University of Vigo, Vigo, Spain, where he is currently working toward the Ph.D. degree in the Department of Electronic Technology.

Since 2007, he has been in the Department of Electronics Technology, University of Vigo. His research interests include switching power converters, grid-connected converters, flexible ac transmission systems, and power quality problems.



Jano Malvar (S'09) received the M.Sc. degree in 2007 from the University of Vigo, Vigo, Spain, where he is currently working toward the Ph.D. degree in the Department of Electronic Technology.

Since 2007, he has been in the Department of Electronics Technology, University of Vigo. His research interests include switching power converters, grid connected converters, flexible ac transmission systems, and power quality problems.



Remus Teodorescu (S'94–A'97–M'99–SM'02) received the Dipl.Ing. degree in electrical engineering from the Polytechnic University of Bucharest, Bucharest, Romania, in 1989, and the Ph.D. degree in power electronics from the University of Galati, Galati, Romania, in 1994.

Since 1998, he has been with the Power Electronics Section, Institute of Energy Technology, Aalborg University, Aalborg East, Denmark, where he is currently a Full Professor. He is the author or coauthor of more than 120 papers, one book, and three patents

(pending). His research interests include design and control of power converters used in renewable energy systems, distributed generation, mainly wind power and photovoltaics, computer simulations, and digital control implementation. He is the Founder and Coordinator of the Green Power Laboratory, Aalborg University, where he is engaged in development and testing of grid converters for renewable energy systems. He is also the Coordinator of the Vestas Power Program.

Prof. Teodorescu was the corecipient of the Technical Committee Prize Paper Award at the IEEE Industry Applications Society (IAS) 1998 Annual Meeting and the Third-ABB Prize Paper Award at the IEEE Optim 2002. He is an Associate Editor of the IEEE TRANSACTIONS ON POWER ELECTRONICS LETTERS and the Chair of the IEEE Danish Joint Industrial Electronics Society/Power Electronics Society/IAS Chapter.



Jesús Doval-Gandoy (M'99) received the M.Sc. degree from the Polytechnic University of Madrid, Madrid, Spain, in 1991, and the Ph.D. degree from the University of Vigo, Vigo, Spain, in 1999.

From 1991 to 1994, he worked at industry. He is currently an Associate Professor in the Department of Electronics Technology, University of Vigo. His research interests include ac power conversion.